View metadata, citation and similar papers at core.ac.uk
brought to you by CORE
provided by Xiamen University Institutional Repository

Photochemistry and Photobiology, 2020, 96: 148–155

Pharmacokinetics and Tissue Distribution of DVDMS-2 in Tumor-bearing Mice

Tingting Li[†1], Haiyan Lv[†2], Liu Yang[1], Jun Xie[1], Cong Liu[1], Peilan Xu[1], Wanyun Li[1], Shengyu Wang[1], Dong Yang[1], Ting Wu*[1], Jianghua Yan*[1] and Fanghong Luo*[1]

[1]Cancer Research Center, School of Medicine, Xiamen University, Xiamen, Fujian, China
[2]Xiamen Mental Health Center, Xiamen Xianyue Hospital, Xiamen, Fujian, China

Received 18 May 2019, accepted 26 September 2019, DOI: 10.1111/php.13171

ABSTRACT

DVDMS-2 is a novel candidate for photodynamic therapy of tumors. The purpose of the present study was to assess the distribution and elimination of DVDMS-2 in mice bearing hepatoma 22 tumors. DVDMS-2 (1, 2 and 4 mg kg^{-1}) was injected intravenously into the mice, extracted from biological tissues and quantified using a fluorescence assay. The data obtained were processed with WinNonlin pharmacokinetic software. The fluorescence assay established for DVDMS-2 quantification was a rapid, reproducible, sensitive and specific method with good linearity. The pharmacokinetics of DVDMS-2 in tumor-bearing mice conformed to a two-compartment model. DVDMS-2 accumulated in tumor tissue to a greater extent than adjacent tissues (skin, muscle) and sustained a relatively high-level concentration 12 to 24 h following administration, which may be the optimal treatment time point. In conclusion, DVDMS-2 selectively accumulated in tumor tissue and was eliminated at a rapid rate in tumor-bearing mice, suggesting that DVDMS-2 may have few side effects, including skin phototoxicity. The present study established the pharmacokinetic characteristics of DVDMS-2, which may be beneficial in future clinical study.

INTRODUCTION

Photodynamic therapy (PDT) has been developed as a novel auxiliary or alternative to traditional cancer treatment. Compared with surgery, radiotherapy and chemotherapy, PDT has high selectivity, is minimally invasive, results in low recurrence rates and may be used multiple times (1). PDT has been used successfully in the clinical treatment of a variety of tumors, including esophageal (2), bladder (3) head and neck (4) and cervical cancer (5), particularly superficial cancer (6). PDT relies on a photosensitizing agent and laser light of appropriate wavelength. Photosensitizers selectively accumulate in tumor tissue and react with laser light, producing reactive oxygen species, including singlet oxygen. These damage several important cellular structures and proteins in cancer cells and lead to death (7–10). PDT is therefore a promising modality in the noninvasive treatment of tumors.

Photosensitizing agents serve a key role in PDT. Photofrin (porfimer sodium) is a first-generation photosensitizer which has achieved remarkable clinical results in recent decades. However, a disadvantage associated with Photofrin is skin photosensitivity that requires patients to avoid light for 4-6 weeks following treatment. Furthermore, Photofrin is a complex mixture, and several of its compounds have not been investigated (11). DVDMS, separated from Photofrin, is a sodium porphyrin dimer sodium salt bonded by an ether bond. DVDMS is a heterogeneous mixture of 3 isomers (DVDMS-1, DVDMS-2 and DVDMS-3), which have equal efficacy (12). However, DVDMS-2, di[1-[6,7-dipropionic acid sodium −1,3,5,8- tetramethyl −2- vinyl -4- porphin] ethyl]ether, is more easily produced and purified and has higher water solubility than the other two isomers (12). DVDMS-2 is a single compound with high photodynamic activity and low skin toxicity that may reduce the side effects associated with Photofrin. The molecular structure of DVDMS-2 is presented in Fig. 1. DVDMS-2 absorbs red light at 628 nm and has been demonstrated to inhibit the growth of tumor cells in vitro and in vivo (13,14) and to induce cell death (15). DVDMS-2, also termed sodium porphyrin, is a potential photosensitizer for the treatment of tumors. However, the pharmacokinetics of DVDMS-2 remain unclear.

The present study investigated hepatocellular carcinoma in BALB/c mice using mouse hepatoma 22 (H22) cells. As PDT is primarily used for the treatment of surface and lumen tumors, a

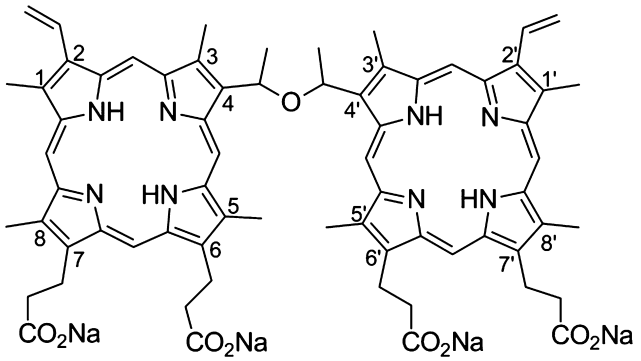

DVDMS-2

Figure 1. Molecular structure of DVDMS-2. Di[1-[6,7- dipropionic acid sodium -1,3,5,8- tetramethyl -2- Vinyl -4- porphin] Ethyl]ether.

*Corresponding authors' emails: luofanghong@xmu.edu.cn (Fanghong Luo); jhyan@xmu.edu.cn (Jianghua Yan) and wuting78@189.cn (Ting Wu)
†These authors contributed equally to this work.
© 2019 American Society for Photobiology

subcutaneous tumor model was used. The pharmacokinetics of DVDMS-2 in tumor-bearing mice was subsequently analyzed using fluorescence spectroscopy. The results obtained in the present study may aid the clinical translation of DVDMS-2.

MATERIALS AND METHODS

Photosensitizer. DVDMS-2 (Qinglong High-Tech Co., Ltd.) was dissolved in 5 % glucose solution to form a 1 mg mL^{-1} solution and stored at −20°C until use.

Experimental animals. Female-specific pathogen-free BALB/c mice were obtained from Shanghai Slac Laboratory Animal Co., Ltd. The mice were 6-8 weeks old with a mean weight of 25 ± 2 g. A cell suspension containing 1×10^6 H22 hepatoma cells was subcutaneously injected into the right axilla of the mice. The animals were administered DVDMS-2 intravenously and protected from light. All experiments were subject to approval by the Animal Care and Use Committee of Xiamen University.

Method validation of DVDMS-2 determination by a fluorescence assay. The concentration of DVDMS-2 in biological samples was determined by a fluorescence assay performed using a LS 55 fluorescence spectrophotometer (Perkin-Elmer, Waltham, Massachusetts) and a 1 cm quartz cuvette. A wavelength range of 550-750 nm and a slit width of 5.0 nm were used for both excitation and emission. The excitation and emission wavelengths were set at 408 and 628 nm, respectively. The specificity, lower limit of quantification, linearity of the calibration curve, precision, accuracy, recovery rate and stability determination of the fluorescence assay were validated.

Plasma pharmacokinetics. Mice with solid tumors were fasted overnight with free access to water. DVDMS-2 dissolved in 5% glucose solution was injected into BALB/c mice via the tail vein at three dosages (1, 2 and 4 mg kg^{-1}), and the mice were subsequently kept in the dark. Blood samples (0.5 mL) were collected from the orbital sinus 5, 10, 20, 30 and 45 min and 1, 2, 6, 12, 24, 48, 72 and 144 h following injection and stored in heparinized tubes. Five animals were studied at each time point. The plasma was separated from blood by centrifugation, protected from light and stored at −20°C until use.

Tissue distribution. Mice with solid tumors were fasted overnight with free access to water. DVDMS-2 dissolved in 5% glucose solution was injected into BALB/c mice via the tail vein at a dose of 2 mg kg^{-1}. Animals were sacrificed by cervical dislocation 5, 10, 20, 30 and 45 min and 1, 2, 6, 12, 24, 48, 72 and 144 h following injection. The heart, lung, liver, kidney, spleen, muscle, skin and tumor tissues were removed, rinsed with saline, blotted dry and stored at −70°C until use. The concentration of the drug in the tissues was measured by the fluorescence assay, using the corresponding tissue from untreated mice as a blank control.

Processing of DVDMS-2 plasma samples. A total of 100 μL plasma was placed into a 5-mL centrifuge tube, followed by the addition of 2.9 mL methanol-PBS (2:1 *v/v*) extracting solution. The solution was mixed for 5 min and centrifuged at 2775 ***g*** for 30 min. The supernatant was removed and placed into another centrifuge tube.

Processing of DVDMS-2 biological tissue samples. A total of 100 mg tissue was placed in a homogenizer, followed by the addition of 1.5 mL phosphate-buffered saline (PBS 10–2 M; pH = 7.4) and fully homogenized. A total of 1.0 mL homogenate was removed and placed into another centrifuge tube. The homogenate was mixed with 2.0 mL methanol and centrifuged at 2775 ***g*** for 30 min. Following centrifugation, the supernatant was removed and placed into another centrifuge tube. The concentration of DVDMS-2 in the supernatant was determined by the fluorescence assay with the excitation and emission wavelengths set at 408 and 628 nm, respectively.

Data analysis. Data are presented as the mean ± standard deviation (X ± S). The pharmacokinetic parameters were obtained using the WinNonlin practical pharmacokinetic calculation program. OriginLab software (version 8.1) was used for statistical analysis.

RESULTS

Plasma pharmacokinetics

The level of DVDMS-2 in tumor-bearing mice plasma, represented by a semilogarithmic plot of mean DVDMS-2 concentration in plasma vs. time following intravenous injection, is shown in Fig. 2. The plasma concentration decreased rapidly in the first 12 h, as is expected for intravenous injection.methanol and centrifuged Compartmental model analysis using WinNonlin software, residual error analysis, correlation coefficient and Akaike information criteria revealed that the pharmacokinetics data are best represented by a two-compartment model. The pharmacokinetic parameters are shown in Table 1. DVDMS-2 plasma levels were described by the following equations: $C(t) = 1.91e^{-0.09t} + 12.25e^{-5.92t}$ ($r = 0.989$) for a dose of 1.0 mg kg^{-1}, $C(t) = 15.71e^{-5.82t} + 5.36e^{-0.16t}$ ($r = 0.998$) for a dose of 2.0 mg kg^{-1} and $C(t) = 21.37e^{-1.63t} + 10.10e{-}0.10t$ ($r = 0.995$) for a dose of 4.0 mg kg^{-1}. DVDMS-2 exhibited a rapid distribution phase and relatively slow elimination phase. Within the dose range studied, the AUC and C0 were dose-dependent. $AUC_{0\to\infty\,(mg\,h^{-1}\,L^{-1})} = 30.384 \times dose_{(mg\,kg^{-1})} - 10.06$ ($r^2 = 0.992; P < 0.05$) and $C_{0\ (mg\,L^{-1})} = 5.6886 \times dose_{(mg\,kg^{-1})} + 8.96$ ($r^2 = 0.995; P < 0.05$). Linear regression coefficients were >0.99, demonstrating a good dose linearity within the dose range used. Consequently, Cl, $t_{1/2}$ and distribution volume at steady state (V_{ss}) were independent of the dose. The *V*ss (range, 0.31-0.34 L kg^{-1}) and the mean residence time (6.8 h and 8.94 h) suggested that DVDMS-2 is widely distributed and is rapidly eliminated.

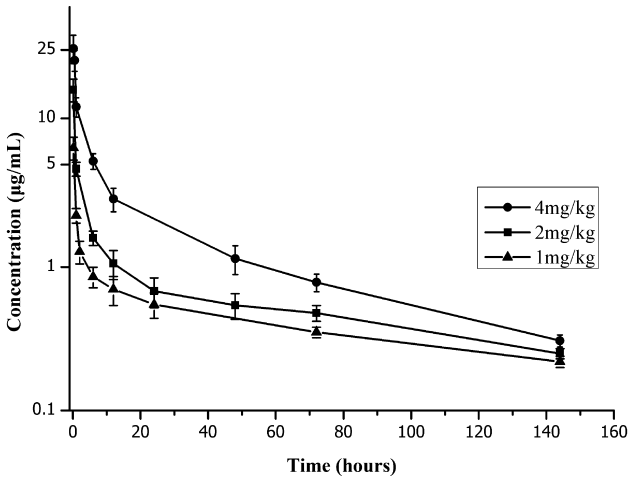

Figure 2. Mean plasma time-concentration curves of DVDMS-2 following a single intravenous dose of 1, 2 and 4 mg kg^{-1} in mice bearing hepatoma 22 solid tumors.

Biodistribution

DVDMS-2 was rapidly distributed to the inner organs and tissues in mice injected with a single dose of 2 mg kg^{-1} (Figs. 3 and 4). DVDMS-2 biodistribution occurred nonuniformly. The peak concentration of DVDMS-2 in healthy inner organs was observed 1-2 h following administration. The peak concentrations in the skin and tumors were observed 6 and 12 h following administration, respectively. The highest concentrations distributed as follows: Liver > lungs > spleen > kidneys > heart > tumor > muscle > skin. At a dose of 2 mg kg^{-1}, the peak concentration in the lungs (24.78 μg g^{-1}) was ~ 20 times higher than the peak concentration in the skin (1.14 μg g^{-1}).

The concentration of DVDMS-2 had rapidly decreased in tissues including the liver, spleen and lungs, and particularly the lung and heart, 6 h following administration. At this time, the

Table 1. Pharmacokinetic parameters following the intravenous administration of DVDMS-2 at single dose of 1, 2 and 4 mg kg^{-1} in tumor-bearing mice.

Pharmacokinetic parameters	Dose: 1 mg kg^{-1} (n = 5)	Dose: 2 mg kg^{-1} (n = 5)	Dose: 4 mg kg^{-1} (n = 5)
Two-compartment model			
Initial concentration (C_0) (mg L^{-1})	14.16	21.07	31.47
Half-life of first compartment ($t_{1/2\alpha}$) (h)	0.11 ± 0.01	0.13 ± 0.02	0.42 ± 0.08
Half-life of second compartment ($t_{1/2\beta}$) (h)	7.68 ± 0.54	4.31 ± 0.56	6.82 ± 1.53
Elimination rate constant from the central compartment (K_{10}) (h^{-1})	0.61 ± 0.08	0.59 ± 0.09	0.27 ± 0.05
Transfer rate constant of compartment 1 to 2 (K_{12}) (h^{-1})	4.64 ± 0.43	3.78 ± 0.42	0.86 ± 0.12
Transfer rate constant of compartment 2 to 1 (K_{21}) (h^{-1})	0.89 ± 0.15	1.59 ± 0.13	0.60 ± 0.07
Peak concentration (C_{max}) (mg L^{-1})	14.43 ± 1.91	21.05 ± 1.38	31.47 ± 3.32
Area under curve ($AUC_{0\rightarrow\infty}$) (mg h^{-1} L^{-1})	23.51 ± 2.72	45.93 ± 5.08	113.07 ± 10.12
Half-life ($t_{1/2}$) (h)	1.13 ± 0.12	1.18 ± 0.19	2.49 ± 0.56
Plasma clearance (Cl) (mL h^{-1} kg^{-1})	0.04	0.06	0.04
Mean residence time (MRT) (h)	10.12 ± 1.91	5.77 ± 1.02	8.77 ± 1.73
Distribution volume at steady state (V_{ss}) (mL kg^{-1})	0.43	0.32 ± 0.03	0.31 ± 0.05

concentration of drug in the lungs had decreased to 40% of the peak concentration. The concentration of drug in heart was at a low level.

The concentration of DVDMS-2 was at a low level in the heart, lungs and kidneys 12 h following administration. The concentration of drug in the liver and spleen had decreased to 30% of the peak concentration. The concentration also decreased in the muscle and skin; however, the peak concentration was reached in tumor tissue.

DVDMS-2 was almost completely eliminated in the majority of tissues 24 h following administration. However, the tumor drug concentration remained >80% of the peak concentration, and the tumor-to-normal tissue ratios were 5 and 7 in the skin and muscle, respectively. DVDMS-2 was completely eliminated in all tissues 48 h following administration.

Method validation

Specificity. The fluorescence emission spectrum of 200 ng mL^{-1} DVDMS-2 dissolved in PBS presented in Fig. 5 shows a characteristic peak at 631 nm. The fluorescence emission spectrum of 200 ng mL^{-1} DVDMS-2 dissolved in methanol-PBS (2:1 *v*/*v*) presented in Fig. 6 shows a characteristic peak at 628 nm. The fluorescence peaks of 200 ng mL^{-1} DVDMS-2 in the two solvents were distinct from impurities. As the fluorescence intensity of DVDMS-2 in methanol-PBS (2:1 *v*/*v*) was >70 times higher than in PBS alone, a mixture of methanol-PBS (2:1 *v*/*v*) was selected as solvent in the current study.

The typical fluorescence spectrums of blank plasma, blank plasma spiked with DVDMS-2 and mouse plasma sample following the intravenous administration of DVDMS-2 are presented in Fig. 7. The results suggested that there was a small but stable interference from endogenous plasma components (Fig. 7A). However, the fluorescence peaks of DVDMS-2 were distinguishable from baseline noise.

Lower limit of quantification. The lower limit of quantification of the fluorescence assay was 10 ng mL^{-1} in biological samples, based on twice the signal-to-noise ratio with background subtraction (Fig. 7B).

Linearity of the calibration curve. DVDMS-2 was diluted with methanol-PBS (2:1 *v*/*v*) to produce a series of standard solutions (0, 10, 20, 40, 80, 100, 200, 400, 800 and 1600 ng mL^{-1}). The fluorescence intensity was measured at excitation and emission wavelengths of 408 and 628 nm, respectively. The regression linear equation obtained was $y = 0.9967C-0.4325$, and the correlation coefficient (R) was 0.9996.

Plasma samples. DVDMS-2 was diluted in blank plasma to produce a series of standard solutions (0, 10, 20, 40, 80, 100, 200, 400, 800 and 1600 ng mL^{-1}). The fluorescence intensity of the standard solutions was measured, and the DVDMS-2 plasma standard curve was constructed. All the fluorescence intensity should be eliminated from blank plasma peak effects. The regression equation of the DVDMS-2 plasma standard curve was $y = 0.6294C$-6.4589 ($R = 0.9966$).

Other biological samples. DVDMS-2 was added to liver tissue homogenate diluted with methanol-PBS (2:1 *v*/*v*) to produce a series of standard solutions, and the fluorescence intensity was measured as described for the plasma samples. All the fluorescence intensity should be eliminated in blank liver tissue peak effects. The regression linear equation of the liver standard curve was $y = 0.3726C$-0.4071 ($R = 0.9961$). Standard curves for the heart, spleen, lungs, kidneys, muscle and skin were established using the aforementioned method. Good linearity in the range of 10–1600 ng mL^{-1} was obtained for all tissues with $R > 0.996$.

Standard curves, correlation coefficients and the linear ranges of DVDMS-2 in tissue samples are presented in Table 2 and Fig. 8.

Accuracy and precision. Six sets of blank plasma and plasma spiked with DVDMS-2 (10, 50 and 200 ng mL^{-1}) were prepared in order to investigate the precision of the assay. The intraday accuracy and precision at concentrations of 10, 50 and 200 ng mL^{-1} DVDMS-2 were determined five times per day. The interday accuracy and precision of DVDMS-2 were determined five times on three different days.

Intraday and interday accuracy and precision of the DVDMS-2 concentration in plasma are presented in Table 3. The reproducibility of the methodology was investigated by examining the intraday and interassay variance. The results revealed that the intra- and interassay relative standard deviation (RSD) was <10%.

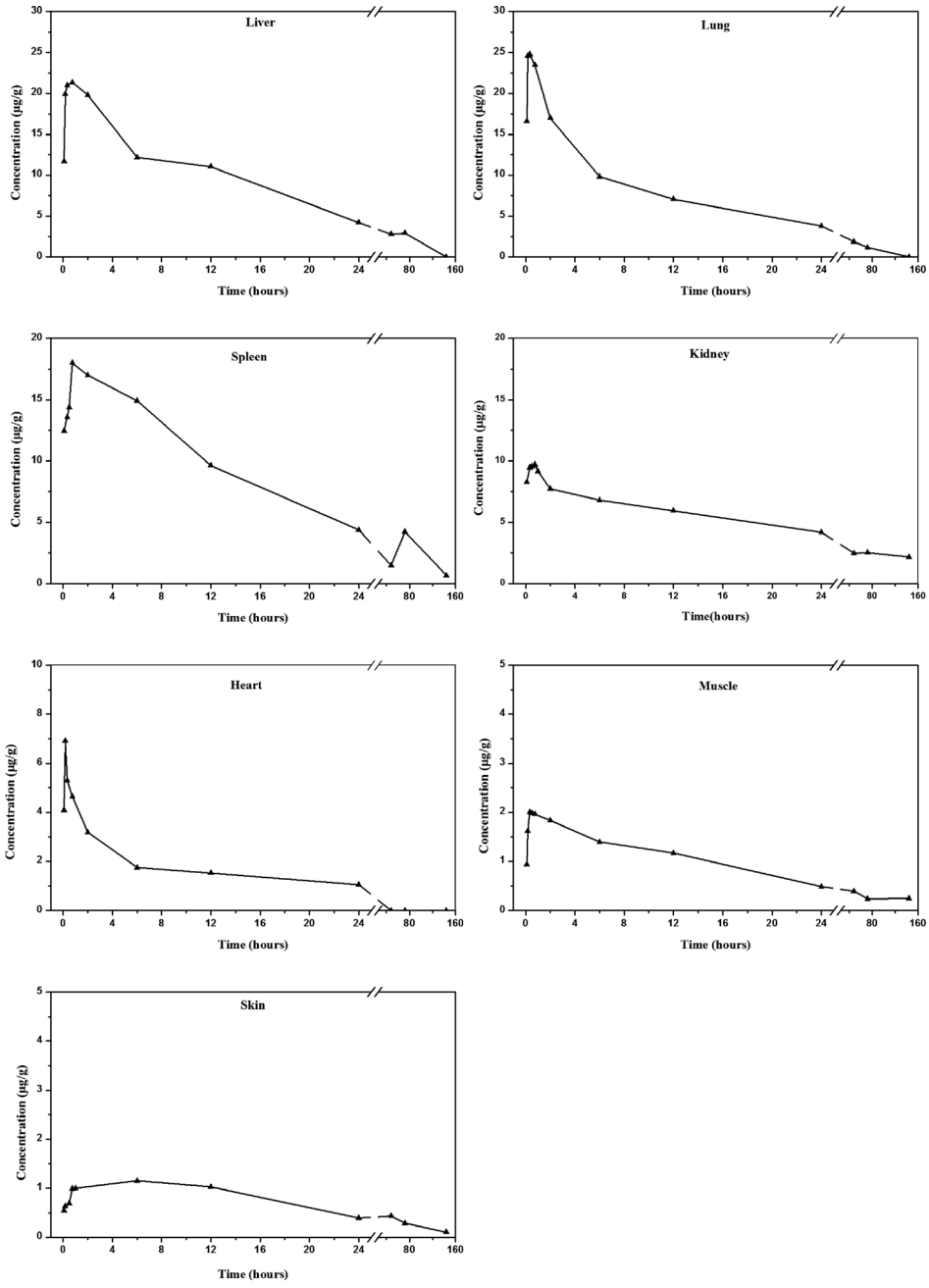

Figure 3. Concentration of DVDMS-2 in the liver, lungs, spleen, kidneys, heart, muscle and skin of mice bearing hepatoma 22 solid tumors at different times following a single intravenous dose of 2 mg kg^{-1}.

Recovery rate and stability. The recovery rate of DVDMS-2 was checked at three quality control levels (10, 50 and 200 ng mL^{-1}) by comparing the fluorescence intensity of DVDMS-2 in extracted plasma or tissue samples with that of DVDMS-2 directly dissolved in standard solutions at the same concentration (Table 4). The recovery rates of DVDMS-2 in plasma over the concentration range of 10–200 ng mL^{-1} ranged between 98.2 and 99.8% with RSD < 5. The recovery rates of DVDMS-2 in tissues were measured in the same way as described for plasma samples, and recovery rates of >80% with RSD < 10% were obtained. DVDMS-2 was recovered in a precise and reproducible manner during the validation experiments.

At ambient temperature, DVDMS-2 was stable for 24.0 h in mouse plasma (RSD = 2.58%). DVDMS-2 was stable when stored at −20°C for a week (RSD = 6.47%).

DISCUSSION

The photosensitizing agent DVDMS-2 is a hydrophilic tetrasodium salt that easily dissolves in alkaline solutions such as PBS (pH 7.4). The peak fluorescence excitation peak of DVDMS-2 is observed at 408 nm. When using PBS as the solvent, the lower limit of quantification of DVDMS-2 was 100 ng mL^{-1}, which was higher than the level of DVDMS-2 in

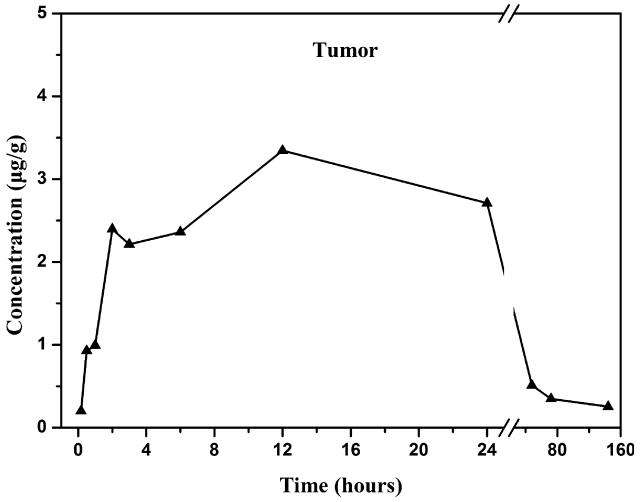

Figure 4. Concentration of DVDMS-2 in hepatoma 22 solid tumors at different times following a single intravenous dose of 2 mg kg^{-1}.

biological samples, and therefore could not be applied for pharmacokinetic studies. However, DVDMS-2 dissolved in methanol-PBS (2:1 *v/v*) exhibits strong fluorescence activity and the lower limit of quantification for DVDMS-2 in the present study was 10 ng mL^{-1}. In order to increase the sensitivity of the DVDMS-2 fluorescence assay, an emission wavelength at 628 nm was selected in the present study. The results revealed that the fluorescence assay using methanol-PBS (2:1 *v/v*) as solvent was a reproducible, sensitive, accurate and specific method to quantify DVDMS-2 with high a recovery rate. The method established in the present study may therefore be applied to investigate the pharmacokinetics of DVDMS-2.

The standard curves constructed in the present study revealed that DVDMS-2 exhibited varying fluorescence intensity in different tissues; however, good linearity was observed in all tissues. For the same concentration of DVDMS-2, the highest fluorescence intensity was observed in serum and skin, and the lowest in spleen. Differences in fluorescence intensity may occur as tissues receive varying blood supplies (16). The fluorescence intensity in all tissues was significantly lower than that observed in methanol-PBS (2:1 *v/v*) solution.

The results obtained in the current study revealed that the concentration of DVDMS-2 in the plasma peaked immediately after intravenous injection and was followed by an exponential decrease. The rate of decline slowed down 6 h following administration. Concentrations of DVDMS-2 came to a low level 24 h following administration and almost disappeared after 72 h. According to the kinetic profile, the plasma elimination of DVDMS-2 fits a two-compartment model. The $t_{1/2\alpha}$ and $t_{1/2\beta}$ were found to be 0.13 h and 5.07 h. Foscan, another photosensitizing agent, exhibits biexponential plasma clearance in mice, with $t_{1/2\alpha}$ and $t_{1/2\beta}$ values of 1.3 and 20.9 h (17), suggesting that DVDMS-2 is more rapidly eliminated than Foscan. The $t_{1/2\alpha}$ and $t_{1/2\beta}$ of DVDMS-2 were shorter than the majority of previously investigated hematoporphyrin derivative drugs. The plasma elimination kinetics of Photofrin II were consistent with a two-compartment model following an intraperitoneal injection of 20 mg kg^{-1}, with $t_{1/2\alpha}$ and $t_{1/2\beta}$ values of 5 and 30 h (18). In cancer patients, the $t_{1/2\beta}$ of Photofrin® was 250 ± 285 h following a single 2 mg kg^{-1} intravenous dose, compared with 415 ± 104 h in healthy subjects (data from the manual of PHOTOFRIN® for Injection). In the present study, DVDMS-2 exhibited rapid distribution and elimination characteristics following intravenous injection in mice and maintained an effective concentration over the time range of light exposure. These characteristics may reduce the accumulation of drug in normal tissues and reduce toxicity.

The V_{ss} of DVDMS-2 was <0.4 L kg^{-1}. The V_{ss} of Photofrin was previously reported to be as high as 2.8 L kg^{-1} (19), suggesting that the distribution of DVDMS-2 was mainly limited to the systemic circulation and blood-rich organs. In the present study, the highest drug concentrations were observed in the liver and lungs, followed by the spleen, kidney and heart. The lowest

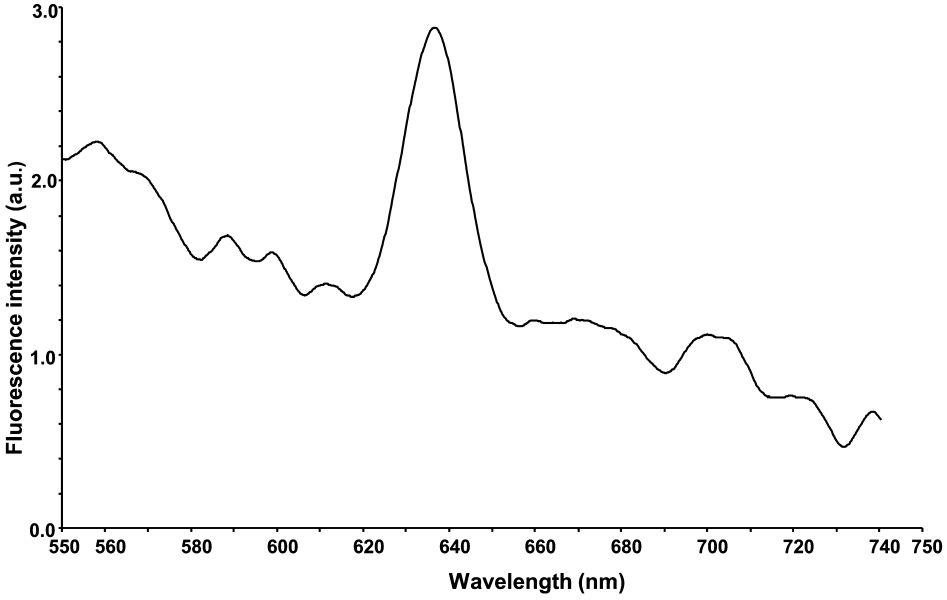

Figure 5. Fluorescence emission spectra of 200 ng mL^{-1} DVDMS-2 dissolved in PBS with the characteristic peak at a wavelength of 631 nm.

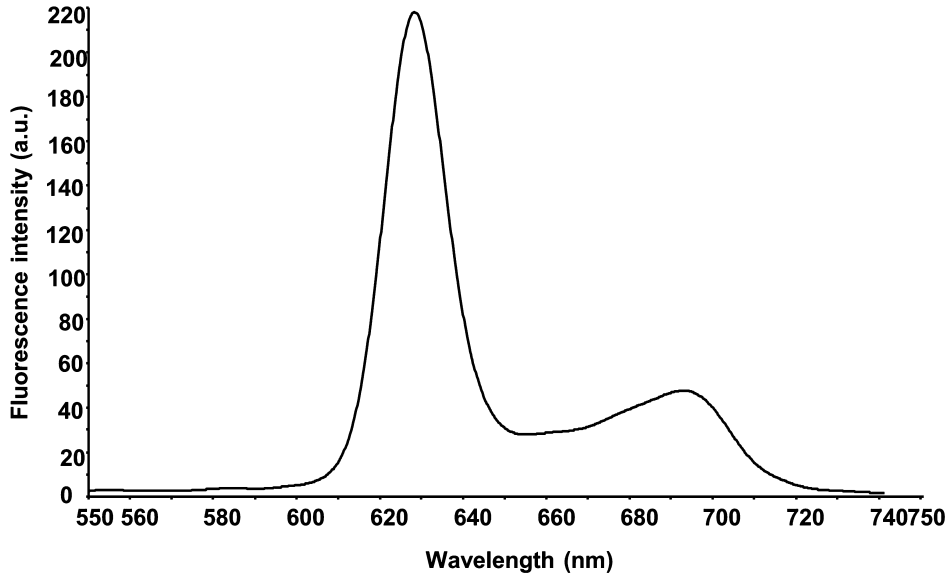

Figure 6. Fluorescence emission spectra of 200 ng mL^{-1} DVDMS-2 dissolved in methanol-PBS (2:1 *v/v*) with the characteristic peak at a wavelength of 628 nm.

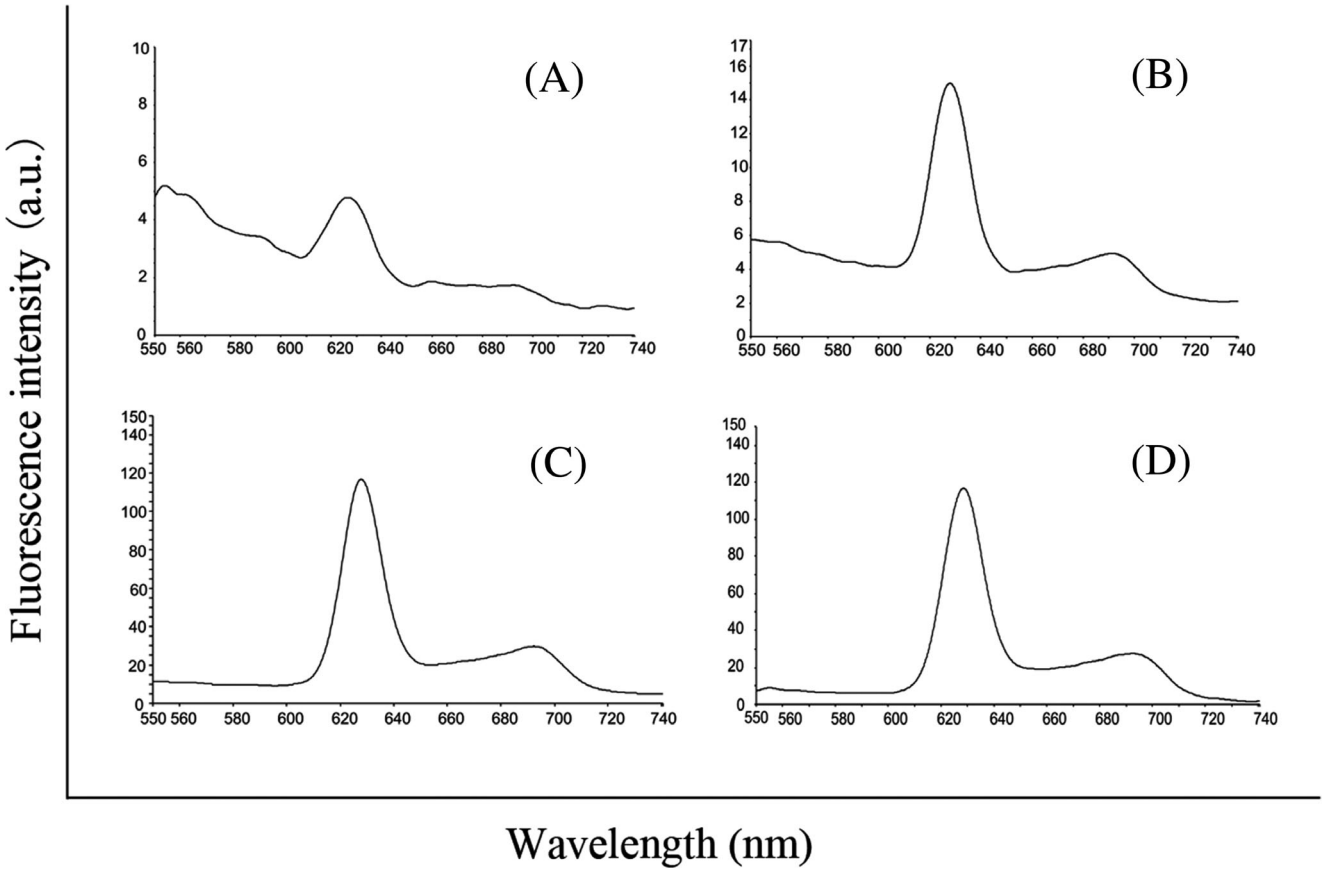

Figure 7. Fluorescence emission spectra of DVDMS-2 in plasma obtained from mice bearing hepatoma 22 solid tumors. The fluorescence excitation spectrum at an emission wavelength of 408 nm exhibited two peaks at wavelengths of 628 nm and 692 nm, respectively. (A) Fluorescence spectrum of blank plasma. (B) The lower limit of quantitation of DVDMS-2 (10 ng mL^{-1}) in plasma. (C) Fluorescence spectrum of DVDMS-2 spiked in plasma at a concentration of 200 ng mL^{-1}. (D) Fluorescence spectrum of a plasma sample containing 195.8 ng mL^{-1} DVDMS-2 following the intravenous administration of 2 mg kg^{-1} DVDMS-2.

concentrations were observed in the skin and muscle. Previous studies have suggested that photosensitizers accumulate in high concentrations due to the specific characteristics of the liver (20,21). Hepatic sinusoidal endothelial cells are highly fenestrated and allow molecules to pass through the blood vessels easily. DVDMS-2 accumulates in the lungs shortly after administration. A previous study reported that high doses of photosensitizing agents resulted in pulmonary hemorrhage and acute interstitial pneumonia (22).

Previous studies demonstrated that several photosensitizers accumulated in components of the reticuloendothelial system (23,24), similar to the results obtained in the current study. The low quantity of DVDMS-2 detected in the skin may decrease the skin photosensitivity associated with photosensitizing agents (13,14). In the present study, the accumulation of DVDMS-2 in tumor tissue gradually increased and peaked 12 h following administration. The DVDMS-2 concentration in tumors was relatively stable 12 to 24 h following administration and was at least 3.2, 2.9 and 3.3 times higher than that in plasma, skin and muscle, respectively. The tumor-to-normal tissue ratio of DVDMS-2 in the current study was higher than that reported for Photofrin (1.7 ± 0.7) (25). The goal of PDT is to achieve the optimal antitumor effect while preserving healthy tissues. The results obtained in the current study suggested that the period between 12 and 24 h following DVDMS-2 administration may be the optimal exposure time. The optimal exposure period following the administration of Photofrin in bile duct cancer is 24–48 h

Table 2. Standard curves, correlation coefficients and linear ranges of DVDMS-2 in tissue samples.

Tissue	Standard curve	Correlation coefficients (R^2)	Linear ranges (ng mL^{-1})
Blood	$y = 0.6294C - 6.4589$	0.9932	10–1600
Heart	$y = 0.3394C - 3.8409$	0.9952	50–400
Liver	$y = 0.3726C - 0.4071$	0.9923	25–1600
Spleen	$y = 0.1574C + 4.9295$	0.9977	10–320
Lung	$y = 0.1985C + 1.179$	0.9947	10–1000
Kidney	$y = 0.3126C - 8.8166$	0.9984	32–500
Muscle	$y = 0.4459C - 2.119$	0.9948	10–200
Skin	$y = 0.6223C - 1.6746$	0.9983	10–200

Table 4. The recovery rate of DVDMS-2 in liver tissue.

Concentration added (ng mL^{-1})	Concentration obtained (ng mL^{-1}) Mean ± SD	Relative recovery (%)
10	9.64 ± 0.43	96.4
50	48.62 ± 1.90	97.2
200	197.46 ± 3.23	98.7

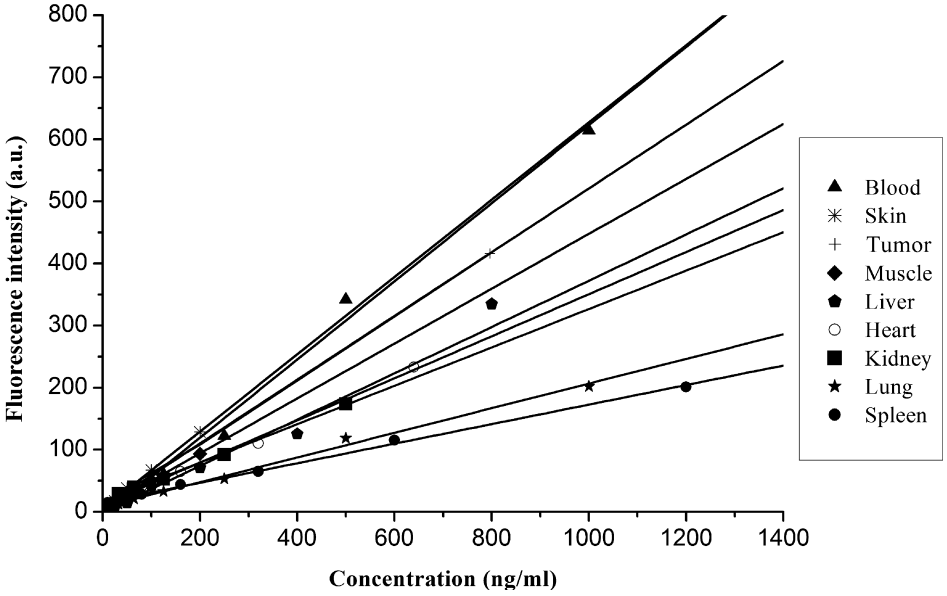

Figure 8. Standard curves of DVDMS-2 in mouse plasma and tissue samples.

Table 3. Intraday and interday accuracy and precision of DVDMS-2 quantification in mice.

Concentration added (ng mL^{-1})	Intraday			Interday Precision RSD (%)
	Concentration obtained (ng mL^{-1}) Mean ± SD	Precision RSD (%)	Accuracy RE (%)	
10	10.20 ± 1.00	9.12	1.95	8.87
50	51.73 ± 4.39	8.97	3.46	2.87
200	205.29 ± 6.08	2.76	2.65	4.17

(25), suggesting that DVDMS-2 may reduce the period of light avoidance prior to laser light irradiation.

CONCLUSION

In conclusion, the fluorescence assay established in the present study was a rapid, constant, sensitive, precise and specific method to determine DVDMS-2 in biological tissues. The results indicated that the pharmacokinetics of DVDMS-2 in tumor-bearing mice was consistent with a two-compartment model. The present study demonstrated that the new novel photosensitizing agent DVDMS-2 preferentially accumulated in H22 tumors compared with the surrounding normal tissues, exhibited rapid clearance from the circulation system and resulted in relatively minor toxicity. Furthermore, the results suggested that the period between 12 and 24 h following administration may be the optimal treatment time point. The results obtained in the present study may guide future studies investigating the effects of DVDMS-2 in vivo.

Acknowledgements—The present study was supported by The National Natural Science Foundation of China (grant no. 81773770) and The Science and Technology Foundation of Fujian Province (grant nos. 2018R1036-1, 2018R1036-3 and 2019R1001-2).

REFERENCES

1. Xiong, W., P. Wang, J. Hu, Y. Jia, L. Wu, X. Chen, Q. Liu and X. Wang (2015) A new sensitizer DVDMS combined with multiple focused ultrasound treatments: an effective antitumor strategy. *Sci. Rep.* **5**, 17485.
2. Kuzyniak, W., J. Schmidt, W. Glac, J. Berkholz, G. Steinemann, B. Hoffmann, E. A. Ermilov, A. G. Gürek, V. Ahsen and B. Nitzsche (2017) Novel zinc phthalocyanine as a promising photosensitizer for photodynamic treatment of esophageal cancer. *Int. J. Oncol.* **50**, 953–963.
3. Lin, T., X. Zhao, S. Zhao, H. Yu, W. Cao, W. Chen, H. Wei and H. Guo (2018) O_2-generating MnO_2 nanoparticles for enhanced photodynamic therapy of bladder cancer by ameliorating hypoxia. *Theranostics.* **8**, 990–1004.
4. Tan, I. B., G. Dolivet, P. Ceruse, V. V. Poorten, G. Roest and W. Rauschning (2010) Temoporfin-mediated photodynamic therapy in patients with advanced, incurable head and neck cancer: a multicenter study. *Head Neck.* **32**, 1597–1604.
5. Choi, M. C., S. G. Jung, H. Park, S. Y. Lee, C. Lee, Y. Y. Hwang and S. J. Kim (2014) Fertility preservation by photodynamic therapy combined with conization in young patients with early stage cervical cancer: a pilot study. *Photodiagnosis Photodyn Ther* **11**, 420–425.
6. Genouw, E., B. Verheire, K. Ongenae, S. S. De, D. Creytens, E. Verhaeghe and B. Boone (2018) Laser-assisted photodynamic therapy for superficial basal cell carcinoma and bowen's disease: a randomised intra-patient comparison between a continuous and a fractional ablative CO_2 laser mode. *J Eur Acad Dermatol Venereol.* **32**, 1897–1905.
7. Kwon, S., Y. Lee, Y. Jung, J. H. Kim, B. Baek, B. Lim, J. Lee, I. Kim and J. Lee (2018) Mitochondria-targeting indolizino [3,2-c] quinolines as novel class of photosensitizers for photodynamic anticancer activity. *Eur J Med Chem* **148**, 116–127.
8. Yuan, S.-X., J.-L. Li, X.-K. Xu, W. Chen, C. Chen, K.-Q. Kuang, F.-Y. Wang, K. Wang and F.-C. Li (2018) Underlying mechanism of the photodynamic activity of hematoporphyrin-induced apoptosis in U87 glioma cells. *Int. J. Mol. Med.* **41**, 2288–2296.
9. Wang, Z.-J., Y.-Y. He, C.-G. Huang, J.-S. Huang, Y.-C. Huang, J.-Y. An, Y. Gu and L.-J. Jiang (1999) Pharmacokinetics, tissue distribution and photodynamic therapy efficacy of liposomal-delivered hypocrellin a, a potential photosensitizer for tumor therapy. *Photochem. Photobiol.* **70**, 773–780.
10. Wang, J.-D., J. Shen, X.-P. Zhou, W.-B. Shi, J.-H. Yan, F.-H. Luo and Z.-W. Quan (2013) Optimal treatment opportunity for mTHPC-mediated photodynamic therapy of liver cancer. *Lasers Med Sci* **28**, 1541–1548.
11. Li, C., K. Zhang, P. Wang, J. Hu, Q. Liu and X. Wang (2014) Sonodynamic antitumor effect of a novel sonosensitizer on S180 solid tumor. *Biopharm. Drug Dispos.* **35**, 50–59.
12. Fang, Q.-C. (2014) Photodynamic therapy for cancer treatment and the new antitumor photosensitizer sinoporphyrin sodium. *Chin J New Drugs* **23**, 1540–1545.
13. Jiang, Z.-H., R. Shi, C. Li and A.-P. Wang (2013) Inhibitory effects of DVDMS-2-based-photodynamic therapy on the growth of tumor in vitro and in vivo. *Teratog. Carcinog. Mutagen.* **25**, 163–167.
14. Wang, X., J. Hu, P. Wang, S. Zhang and Q. Liu (2015) Analysis of the in vivo and in vitro effects of photodynamic therapy on breast cancer by using a sensitizer, sinoporphyrin sodium. *Theranostics* **5**, 772–786.
15. Li, L., H. Wang, H. Wang, L. Li, P. Wang, X. Wang and Q. Liu (2017) Interaction and oxidative damage of DVDMS to BSA: a study on the mechanism of photodynamic therapy-induced cell death. *Sci. Rep.* **7**, 43324.
16. Ziegler, V. G., K. Plaetzer, D. Stahl and B. Krammer (2011) Photodynamic treatment for the selective depletion of circulating tumor cells in human mononuclear cell-enriched blood preparations. *Photodiagnosis Photodyn Ther* **8**, 138–138.
17. Mody, T. D. and J. L. Sessler (2001) Texaphyrins: a new approach to drug development. *J Porphyr Phthalocyanines* **5**, 134–142.
18. Pandey, R. K. (2013) Recent advances in photodynamic therapy. *J Porphyr Phthalocyanines.* **4**, 368–373.
19. Bellnier, D. A., W. R. Greco, G. M. Loewen, H. A. R. Oseroff and T. J. Dougherty (2010) Clinical pharmacokinetics of the PDT photosensitizers porfimer sodium (Photofrin), 2-[1-hexyloxyethyl]-2-devinyl pyropheophorbide-a (Photochlor) and 5-ALA-induced protoporphyrin IX. *Lasers Surg Med.* **38**, 439–444.
20. Paszko, E., C. Ehrhardt, M. O. Senge, D. P. Kelleher and J. V. Reynolds (2011) Nanodrug applications in photodynamic therapy. *Photodiagnosis Photodyn. Ther.* **8**, 14–29.
21. Peng, Q., J. Moan, M. Kongshaug, J. F. Evensen, H. Anholt and C. Rimington (1991) Sensitizer for photodynamic therapy of cancer: a comparison of the tissue distribution of Photofrin II and aluminum phthalocyanine tetrasulfonate in nude mice bearing a human malignant tumor. *Int J Cancer* **48**, 258–64.
22. Razum, N. J., A. B. Snyder and D. R. Doiron (1996) SnET2: Clinical update. *Proc SPIE.* **2675**, 43–46.
23. Stewart, F. A., P. Cramers, M. Ruevekamp, H. Oppelaar, O. Dalesio and P. Baas (2003) Foscan (R) uptake and tissue distribution in relation to photodynamic efficacy. *Brit J Cancer* **88**, 283–290.
24. Wang, G. J., R. Wang, H. P. Hao, H. T. Xie, M. J. Xu, W. Wang, H. He and X. Y. Li (2008) Pharmacokinetics, tissue distribution and excretion of a new photodynarnic drug deuxemether. *J. Photochem. Photobiol. B-Biol.* **90**, 179–186.
25. Pahernik, S. A., M. Dellian, F. Berr, A. Tannapfel, C. Wittekind and A. E. Goetz (1998) Distribution and pharmacokinetics of Photofrin in human bile duct cancer. *J. Photochem. Photobiol. B-Biol.* **47**, 58–62.